Journal of Thermal Analysis and Calorimetry, Vol. 81 (2005) 563–567

MIXING STATE OF AMPHIPHILIC DI-BLOCK COPOLYMER/HOMOPOLYMER BLENDS

S. Y. Jung[1], *T. Yamada*[1], *H. Yoshida*[1,2*] *and T. Iyoda*[2,3]

[1]Department of Applied Chemistry, Graduate School of Engineering, Tokyo Metropolitan University, 1-1 Minami-Osawa, Hachiouji, Tokyo 192-0397 Japan
[2]CREST (JST)
[3]Chemical Research Laboratory, Tokyo Institute of Technology, 4259 Nagatsuta-cho, Midori-ku, Yokohama 226-8503, Japan

The mixing state of amphiphilic di-block copolymers consisted of poly(ethylene oxide) and poly(methacrylate) having azobenzene moieties in the side chains $p(EO)_{114}pMA(Az)_{24}$ and poly(ethylene oxide) $p(EO)_{114}$ was investigated from the viewpoints of isothermal crystallization and nano-scale ordered structure. The chemical potential, which required establishing the constant crystal growth rate, decreased with the p(EO) content up to 60%. The hexagonal packed cylinder structure was observed for the blends with the p(EO) content up to 60% and the lattice spacing of (100) and (110) planes increased with the p(EO) content up to 60%. The blends of amphiphilic $p(EO)_{114}pMA(Az)_{24}$ and $p(EO)_{114}$ were miscible without in the p(EO) content below 60%.

Keywords: *blend, di-block copolymer, hexagonal packed cylinder, isothermal crystallization, micro-phase separation*

Introduction

The self-assembly of block copolymers through micro-phase separation of block components as the results of repulsive interaction between copolymer contents are well investigated [1–6]. These self-assembled di-block copolymers form the nano-scale ordered morphologies such as spheres, cylinders, bi-continuous gyroid, lamellae as the equilibrium structure depending on the relative volume fractions of components and temperature [7, 8]. Both Flory–Huggins interaction parameter between copolymer components (χ) and total degrees of polymerization of AB type copolymer ($N=n+m$ in A_nB_m) influence strongly on the nano-scale structure from thermodynamic viewpoint [9, 10].

We have reported the nano-scale ordered structure and phase transitions for amphiphilic di-block copolymer consisted of hydrophilic poly(ethylene oxide) and hydrophobic poly(methacrylate) having azobenzene moieties in ester groups ($p(EO)_npMA(AZ)_m$) [11–13]. The amphiphilic di-block copolymers $p(EO)_npMA(AZ)_m$ form the ordered hexagonal-packed p(EO) cylinder structure selectively in the wide ranges of both copolymer content and temperature. The order of hexagonal packed cylinder structure is affected by annealing temperature [11, 12]. From the polymerization difficulty of $p(EO)_n$ $pMA(AZ)_m$ with high degree of polymerization of p(EO), the nano-scale ordered structure of $p(EO)_npMA(AZ)_m$ having higher p(EO) content had not investigated yet. In this study, the nano-scale ordered structure and the mixing state of blends of $p(EO)_{114}pMA(AZ)_m$ and homo $p(EO)_{114}$ polymer having same degree of polymerization of p(EO) were discussed. The nano-scale ordered structure changes in the blend systems of di-block copolymer and homopolymer are well investigated for lamellar structure of di-block copolymers [14–16] and tri-block copolymers [17].

For the blend system, the evaluation of mixing state is important to discuss the structure caused by the micro-phase separation of block copolymer. Generally, the miscibility of blends including crystalline polymer is evaluated from the relationship between melting temperature and blend content. We have proposed the evaluation method of mixing from the viewpoint of crystallization process [18]. The nucleation and crystal growth rates for miscible blends depended on the blend content, however, these rates were independent on the blend content for immiscible blends [19–21]. In this study, the mixing state of di-block copolymer and homopolymer blends were evaluated by the analysis of crystallization dynamics at isothermal conditions and of nano-scale ordered structure.

Experimental

Materials and preparation of blends

The amphiphilic di-block copolymer, $p(EO)_{114}$ $pMA(Az)_{24}$ (Scheme 1) and poly(ethylene oxide) homopolymer, $p(EO)_{114}$ were used through this study. The blends of $p(EO)_{114}pMA(Az)_{24}$ and $p(EO)_{114}$ were

* Author for correspondence: yoshida-hirohisa@c/metro-u.ac.jp

1388–6150/$20.00

Akadémiai Kiadó, Budapest, Hungary
Springer, Dordrecht, The Netherlands

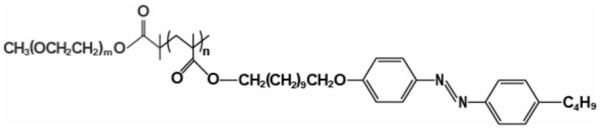

Scheme 1. Molecular structure of $p(EO)_mpMA(Az)_n$ block copolymer

prepared by solution casting method from toluene solution, and were dried under reduced pressure. The p(EO) content of blends were 40 (B4), 50 (B5), 60 (B6), 70 (B7), 80 (B8) and 90 (B9) in mass %. Before DSC and SAXS measurements, all samples containing $p(EO)_{114}pMA(Az)_{24}$ were annealed at 140°C for 24 h in order to form the equilibrium nano-scale ordered structure.

Differential scanning calorimetry (DSC)

The phase transition behaviors and the isothermal crystallization were carried out by a differential scanning calorimeter (DSC6200, Seiko Instruments Co. Ltd) equipped with a cooling apparatus in dry nitrogen gas atmosphere. The sample mass and scanning rate were about 3 mg and 10 K min^{-1}, respectively. The phase transition temperatures of melting and crystallization were employed as the on-set temperature at 10 K min^{-1}. The isothermal crystallization was carried out at predetermined crystallization temperatures (T_c) after cooling at 10 K min^{-1} from 60°C. After isothermal crystallization, the melting temperature (T_m) was obtained by heating at 10 K min^{-1} from T_c to 60°C.

Small-angle X-ray scattering (SAXS)

The SAXS measurements were carried out at the beam line 10C at Photon Factory, High Energy Acceleration Organization, Tsukuba, Japan. The wavelength of monochromatic X-ray was 0.1488 nm. The distance between sample and detector (PSPC, Rigaku Co. Ltd, 512 channels) was 860 mm, which covered 1.02 nm$<s^{-1}=q/2\pi=\lambda/2\sin\theta<$60.8 nm.

Results and discussion

Figure 1 shows the DSC curves of $p(EO)_{114}$, $p(EO)_{114}pMA(Az)_{24}$ and blend systems on second heating (Fig. 1a) and second cooling process (Fig. 1b). In the case of $p(EO)_{114}pMA(Az)_{24}$, on heating (Fig. 1a), the endothermic peaks at 37 and 111.7°C corresponded to the melting of p(EO) and the isotropic transition of azobenzene moieties, respectively. The isotropic transition temperature has no influence by blending with $p(EO)_{114}$. The double melting peaks was observed at

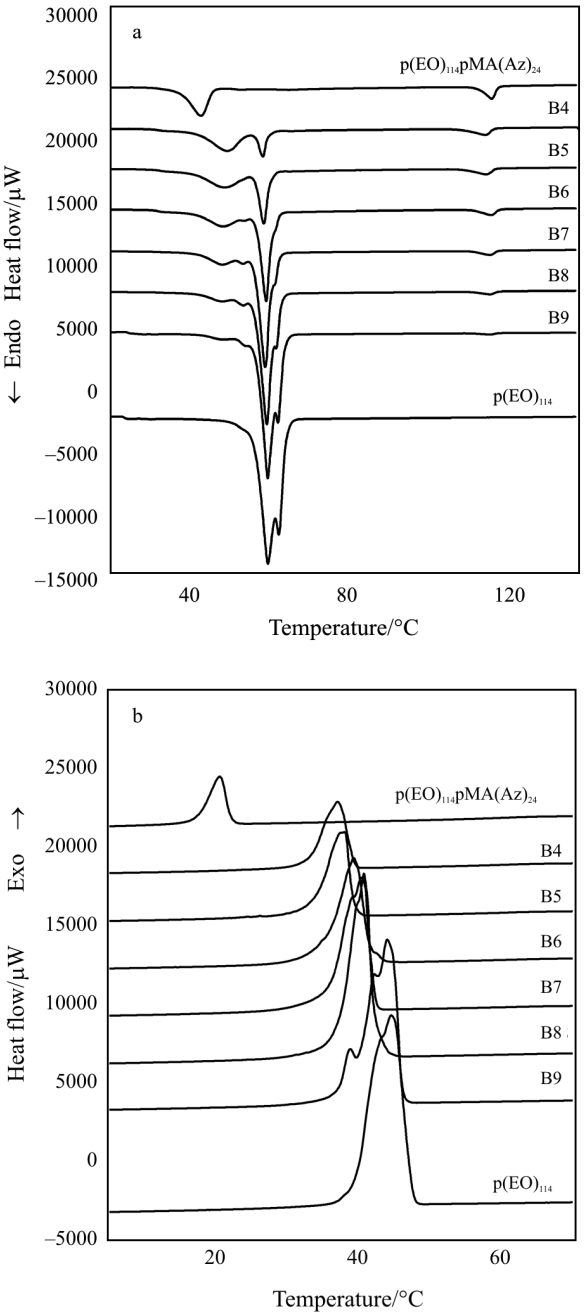

Fig. 1 DSC curves of homo-polymer $p(EO)_{114}$, copolymer $p(EO)_{114}pMA(Az)_{24}$ and blend systems (B4, B5, B6, B7, B8 and B9) on a – second heating and b – second cooling at ± 10 K min^{-1}

56°C for $p(EO)_{114}$, the mechanism of double peaks was not clear. For blend samples, two types of melting peak of p(EO) were observed, one was due to the melting of p(EO) in di-block copolymer and the other was due to the melting of $p(EO)_{114}$. The melting temperature of the former endothermic peak shifted from 37 to 42°C with the increase of $\phi_{p(EO)}$ and leveled off above 70%. The melting temperature of the latter main peak had no influenced by blending, however, the double melting peaks became to the single peak by

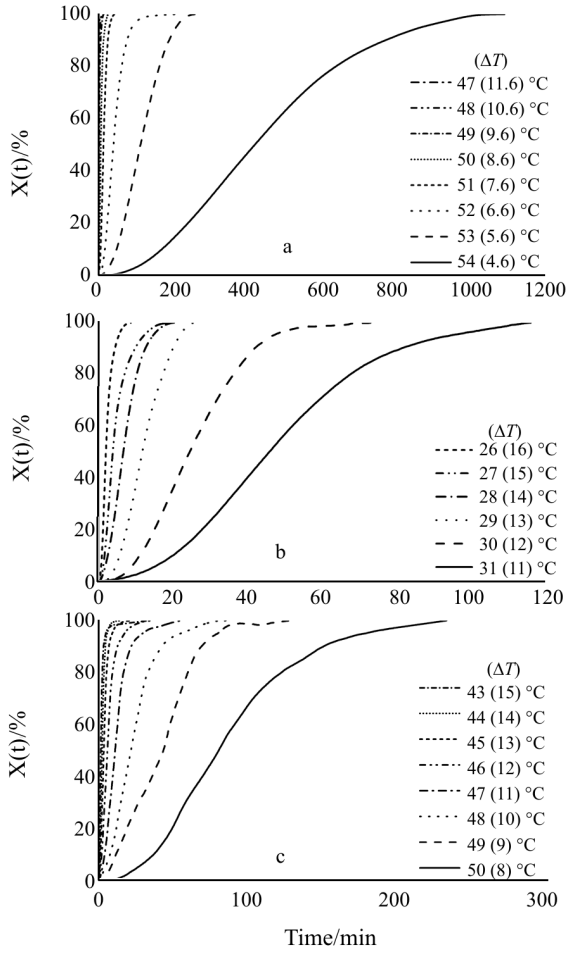

Fig. 2 Changes of relative crystallinity X(t) with time at various crystallization temperatures for a – $p(EO)_{114}$, b – $p(EO)_{114}pMA(Az)_{24}$ and c – B4

blending with $p(EO)_{114}pMA(Az)_{24}$. These results indicated that the p(EO) domains of di-block copolymer mixed with $p(EO)_{114}$ in the $\phi_{p(EO)}$ range up to 70%.

For the cooling process, the exothermic peak due to crystallization of $p(EO)_{114}$ shifted from 48 to 39°C continuously with the decrease of $\phi_{p(EO)}$ until 40%. The crystallization peak of $p(EO)_{114}$ accompanying shoulders at the lower temperature side were observed for $p(EO)_{114}$ and the blends having higher p(EO) content. The crystallization of $p(EO)_{114}$ was disturbed by blending with $p(EO)_{114}pMA(Az)_{24}$. These results suggested that $p(EO)_{114}$ mixed with di-block copolymer in some extent.

From the exothermic peak observed during the isothermal crystallization, the relative degree of crystallinity, *X(t)* was obtained as follows.

$$X(t)=\frac{\Delta H_t}{\Delta H_{exo}} \quad (1)$$

where, ΔH_{exo} and ΔH_t indicate the total exothermic enthalpy and the partial enthalpy at time *t*, respectively. The *X(t)* changes at various crystallization temperatures for homo-polymer $p(EO)_{114}$, di-block copolymer $p(EO)_{114}pMA(Az)_{24}$ and the blend B4 are shown in Fig. 2a, b and c, respectively. The equilibrium melting temperature T_m^0, which was obtained by Hoffman–Weaks plot of T_c and T_m of $p(EO)_{114}$ and p(EO) in $p(EO)_{114}pMA(Az)_{24}$ were 58.6 and 42.4°C, respectively. Numbers in parentheses indicate the degree of super-cooling ($\Delta T=T_m^0-T_c$). As the isothermal crystallizations of blends examined in the temperature range above 40°C which corresponded to the crystallization range for $p(EO)_{114}$, 58.6°C was used as T_m^0 value of blends. From Fig. 2, the time required to approach at $X(t)=0.5$ from the start time of exothermic peak ($t_{0.5}$) was obtained for all samples. The crystal growth rate (G^*) was defined by the reciprocal of $t_{0.5}$.

The relationship between G^* and ΔT for all samples is shown in Fig. 3. Temperature dependence of G^* is described by the following equation [22].

$$G^*=G_0\left(=\frac{\Delta E}{RT}=K\frac{T_m}{RT\Delta T}\right) \quad (2)$$

Here, G_0, ΔE, R and K indicate a pre-exponential parameter, an activation energy for molecular diffusion through interface between amorphous and crystalline regions, gas constant and a constant including surface free energy of crystallites, respectively. Temperature dependence of G^* for all samples shown in Fig. 3 were described by Eq. (2), therefore, the crystallization mechanism of p(EO) in di-block copolymer, homopolymer and these blends were same. At given ΔT, G^* decreased with the decrease of $\phi_{p(EO)}$. The ΔT value where G^* approached to a constant value ($G^*=0.07$ min^{-1}) was determined from Fig. 3.

The chemical potential difference ($\Delta\mu$) required to establish a constant crystallization rate from the molten state is described as follows.

$$\Delta\mu=\Delta_{fus}h(\Delta T/T_m^0) \quad (3)$$

Here, $\Delta_{fus}h$ is the fusion enthalpy of molecule. The $\Delta T/T_m^0$ values obtained from Fig. 3 at a constant G^* are plotted *vs.* $\phi_{p(EO)}$ in Fig. 4. The $\Delta T/T_m^0$ values decreased linearly with increasing $\phi_{p(EO)}$ up to 60% and leveled off above 60%. The linear relationship between $\Delta T/T_m^0$ and blend content is obtained for the miscible blend systems, poly(vinylidenefluoride)/poly(methylmethacrylate) [19], poly(vinylidenfluoride)/poly(ethylmethacrylate) [19], atactic poly(styrene)/syndiotactic poly(styrene) [20] and nylon 66/nylon 48 [21].

The result shown in Fig. 4 suggested that $p(EO)_{114}$ miscible in p(EO) domain of $p(EO)_{114}pMA(Az)_{24}$ in the $\phi_{p(EO)}$ range from 30 to 60%.

The nano-scale ordered structure for blend samples through micro-phase separation was determined by small-angle X-ray scattering (SAXS). Figure 5

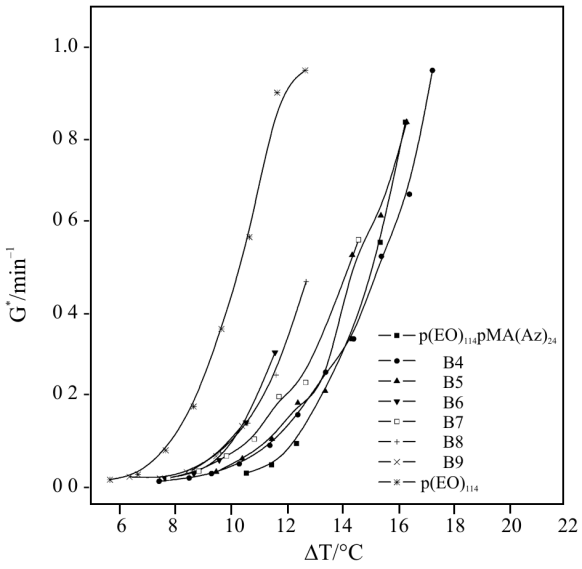

Fig. 3 Relationship between crystal growth rate (G^*) and degree of super-cooling (ΔT) for homo-polymer $p(EO)_{114}$, copolymer $p(EO)_{114}pMA(Az)_{24}$ and blend systems (B4, B5, B6, B7, B8 and B9)

shows the SAXS profiles of copolymer $p(EO)_{114}pMA(Az)_{24}$ and blend systems. The SAXS peaks observed at scattering vector in the relation of $1:\sqrt{3}:\sqrt{4}:\sqrt{7}$, which indicated that the nano-scale order structure was a hexagonal packed cylinder for $p(EO)_{114}pMA(Az)_{24}$ and blends in the $\phi_{p(EO)}$ range below 60%. With increasing, $\phi_{p(EO)}$ the high-order SAXS peaks ($\sqrt{4}$ and $\sqrt{7}$) became smaller, the SAXS

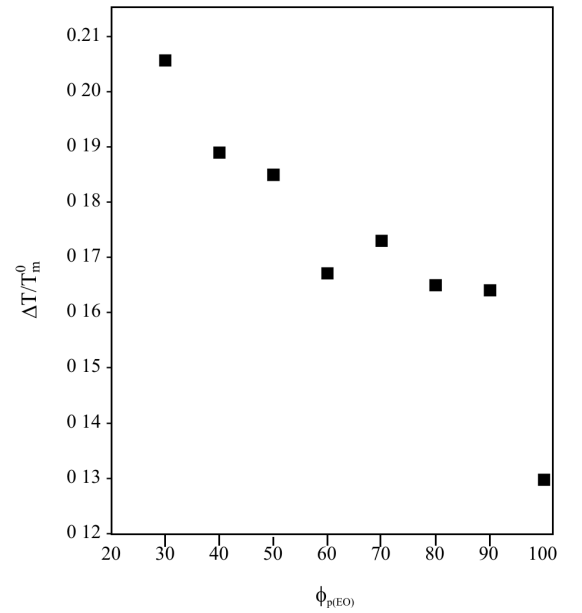

Fig. 4 Blend content ($\phi_{p(EO)}$) dependency of chemical potential function evaluated at crystal growth rate (G^*=0.07 min^{-1})

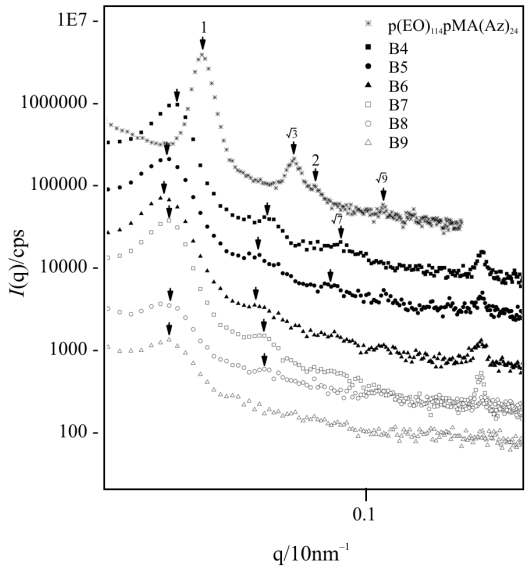

Fig. 5 SAXS profiles of copolymer $p(EO)_{114}pMA(Az)_{24}$ and blend systems (B4, B5, B6, B7, B8 and B9)

profiles of the blends with $\phi_{p(EO)}$ above 70% has no high-order peaks corresponding to $\sqrt{4}$ and $\sqrt{7}$. These results suggested that the hexagonal cylinder structure was kept for the blends in the $\phi_{p(EO)}$ range below 60%, however, the order of hexagonal cylinder structure decreased with $\phi_{p(EO)}$. The blend B9 showed only the first SAXS peak. The lattice distance of (100) and (110) planes are plotted *vs.* $\phi_{p(EO)}^{1/3}$ in Fig. 6. As the blend content was shown in mass %, the power low of

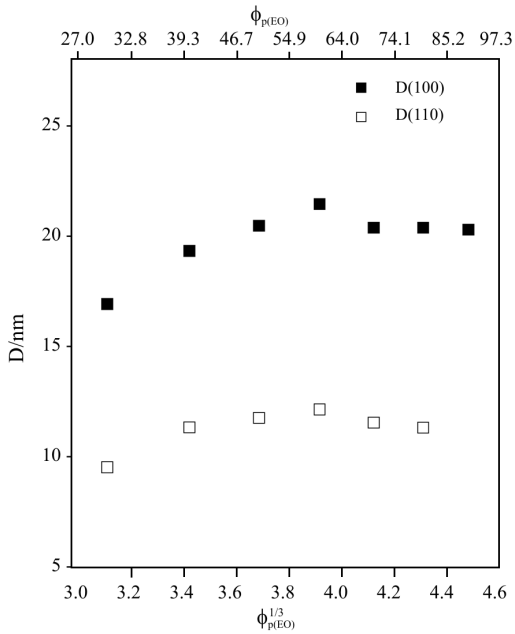

Fig. 6 Relationship between $\phi_{p(EO)}^{1/3}$ and space distances of (100) and (110) plane of hexagonal cylinder structure for homo-polymer $p(EO)_{114}$, copolymer $p(EO)_{114}pMA(Az)_{24}$ and blend systems (B4, B5, B6, B7, B8 and B9)

weight increment contribution on the lattice distance should be explained by 1/3 for the isotropic structure. Although the hexagonal packed cylinder was anisotropic structure, both lattice distance increased linearly up to 60% and approached to 21.4 and 12.2 nm, respectively. These facts suggested that the blend of $p(EO)_{114}$ increased the cylinder distance effectively, which was the results of the miscibility of $p(EO)_{114}$ in p(EO) cylinder of $p(EO)_{114}$ $pMA(Az)_{24}$. The SAXS results shown in Fig. 6 agreed with the isothermal crystallization results in Fig. 4.

Conclusions

The thermal properties and the nano-scale ordered structure of $p(EO)_{114}pMA(Az)_{24}/p(EO)_{114}$ blends were investigated by DSC and SAXS. The crystallization temperature depression of $p(EO)_{114}$ by blending of $p(EO)_{114}pMA(Az)_{24}$ was observed for all blend samples. From the isothermal crystallization, the chemical potential required to establish the constant crystal growth rate (G^*=0.07 min^{-1}) decreased linearly with the increase of $\phi_{p(EO)}$ up to 60%. The hexagonal packed cylinder structure caused by the micro phase separation of $p(EO)_{114}pMA(Az)_{24}$ was observed for the blends with $\phi_{p(EO)}$ up to 60 %. The lattice spacing of (100) and (110) planes of hexagonal phase increased linearly with the increase of $\phi_{p(EO)}^{1/3}$ up to 3.91%. From these results, $p(EO)_{114}$ was miscible in the p(EO) cylinder of $p(EO)_{114}pMA(Az)_{24}$ in the $\phi_{p(EO)}$ region between 30 and 60%.

References

1 D. J. Meier, J. Polym. Sci., C, 26 (1969) 81.
2 E. Helfand, Macromolecules, 8 (1975) 552.
3 M. W. Matsen and F. S. Bates, J. Chem. Phys., 106 (1997) 2436.
4 H. Tanaka, H. Hasegawa and T. Hashimoto, Macromolecules, 24 (1991) 4378
5 L. Zhu, B. H. Calhoun, Q. Ge, R. P. Quirk and S. Z. D. Cheng, Macromolecules, 34 (2001) 1244.
6 D. A. Hadjuk, Macromolecules, 28 (1995) 2570.
7 Developments in Block copolymers; I. Goodman, Ed., Applied Science, New York 1982; Vol. 1.
8 F. S. Bates and G. H. Fredrickson, Physics Today, 52 (1999) 32.
9 M. W. Matsen and F. Bates, Macromolecules, 29 (1996) 1091.
10 V. Abetz, 'Supramolecular Polymer', Edit. by A. Ciferri, Chapter 6, Mercel Dekker Inc. New York 2000.
11 Y. Tian, K. Watanabe, X. Kong, J. Abe and T. Iyoda, Macromolecules, 35 (2002) 3739.
12 K. Watanabe, Y. Tian, H. Yoshida, S. Asaoka and T. Iyoda, Trans. Materials Res. Soc. Jpn., 28 (2003) 553.
13 H. Yoshida, K. Watanabe, R. Watanabe and T. Iyoda, Trans. Materials Res. Soc. Jpn., 28 (2003) 553.
14 B. Ptaszynski, J. Terrisse and A. Skoulious, Macromol. Chem., 176 (1975) 3438.
15 T. Hashimoto, H. Tanaka and H. Hasegawa, Macromolecules, 23 (1990) 4378.
16 K. I. Winey, E. L. Thomas and L. J. Fetters, Macromolecules, 24 (1991) 6182.
17 A. Noro, M. Iinuma, J. Suzuki, A. Takano and Y. Matsushita, Macromolecules, 37 (2004) 3804.
18 H. Sasaki, P. K. Bala and H. Yoshida, Polymer, 25 (1995) 4805.
19 H. Yoshida, G. Z. Zhang, T. Kitamura and T. Kawai, J. Therm. Anal. Cal., 64 (2001) 577.
20 T. Watanabe, G. Z. Zhang, H. Yoshida and T. Kawai, J. Therm. Anal. Cal., 72 (2003) 57.
21 G. Z. Zhang, H. Yoshida and T. Kawai, Thermochim. Acta., 416 (2004) 79.
22 J. D. Hoffman, G. T. Davis and J. I. Lauritzen, Treaties on Solid State Chem, Vol. 3, Chap. 7, Plenum Press, New York 1976.

DOI: 10.1007/s10973-005-7082-0